Electrochemistry Communications 155 (2023) 107582

Contents lists available at ScienceDirect

Electrochemistry Communications

journal homepage: www.elsevier.com/locate/elecom

Carbon modified silver thin-film catalysts for electrochemical reduction of CO_2 to syngas with tunable H_2/CO ratio

Kim Robert Gustavsen, Erik Andrew Johannessen, Kaiying Wang *

Department of Microsystems, University of South-Eastern Norway, Horten 3184, Norway

ARTICLE INFO

Keywords:
AgC
Carbon doped silver
electrochemical CO_2 reduction
Silver catalyst
Syngas production
Thin films

ABSTRACT

This study investigates carbon (C)-modified silver (Ag) thin film catalysts for electrochemical syngas production. The Ag-C catalyst is synthesized using a co-deposition process with separate C and Ag sputtering targets. It is found that co-deposition with C increases nucleation rate during film growth, which reduces particle size and increases the surface area, as well as increasing the selectivity for the hydrogen evolution reaction (HER). A 10-fold improvement in the geometric current density is obtained for the Ag-C thin film relative to Ag due to a high abundance of active sites, and a H_2/CO ratio between 1.4 and 2.5 is attained within the potential range of − 0.6 to − 1.0 V. vs RHE. Thus, regulating the C concentration allows the H_2/CO ratio to be tuned while maintaining a surface architecture that permits large geometric current densities, both being desirable properties for catalysts used in syngas applications.

1. Introduction

The electrochemical reduction of carbon dioxide through the CO_2 reduction reaction (CO2RR) could help meet future energy demands by generating value-added liquid fuels and chemical feedstocks that are carbon neutral. One challenge lies in activating the CO_2 molecule, which requires high overpotentials, as well as being in the potential range of the hydrogen evolution reaction (HER). The result is a low faradaic efficiency (FE) for the CO_2 reduction process. Despite significant efforts to suppress HER and activate CO_2 molecules through catalyst design, there remains an urgent need for cost effective stable catalysts with high FE and selectivity for CO_2. One potential solution is to permit the HER process to proceed and to combine this with CO2RR to produce syngas with adjustable H_2/CO ratios. Syngas is commonly generated from the energy-intensive water–gas shift reaction, which utilizes CO and water at high temperatures to produce H_2 at desired ratios [1]. However, the process emits CO_2 as a byproduct, which raises environmental concerns. Being able to fine tune the H_2/CO ratio of the syngas allows the mixture to be used directly in existing thermocatalytic processes such as the Fischer-Tropsch (FT) and direct methanol synthesis, eliminating the need for the water gas shift reaction [2].

Designing catalysts for syngas formation requires the use of group 2 transition metals in the CO2RR. These produce CO as their main product due to their inherent weak binding of CO, which permits efficient desorption of the CO molecule [3]. Among these transition metals, silver (Ag), gold (Au), and palladium (Pd) have been explored as potential catalysts for production of syngas [2,4–8], of which Ag is considered the most viable from an economic perspective due to its significantly lower cost compared to Au and Pd. However, Ag exhibits the lowest catalytic activity of the three and often requires larger overpotentials to achieve satisfactory reaction rates. Thus, to utilize Ag as a catalyst for syngas formation the reaction rate must be enhanced, the H_2/CO ratio must be controlled, and preferably the Ag content should be minimized to further reduce the cost. To address these challenges, nanostructured Ag catalysts have been employed [6,9], which can maximize the exposed surface area to increase the number of active sites, which in turn boost reaction rates at the same time as the Ag loading is reduced. In order to achieve this, carbon (C) and its derivatives are often used as a support for Ag to make use of its porous structure [10]. In addition, the H_2/CO production ratio can be controlled by adjusting the Ag loading [11]. Therefore, from this viewpoint, the creation of Ag-C thin films is appealing as it allows for control over C concentration and film thickness. This could help minimize the Ag loading, thus reducing costs. Moreover, thin film deposition can readily be scaled up, and it eliminates the use of binders that are necessary for fixing Ag nanostructures to electrodes, which can block access to active sites [10].

* Corresponding author.
E-mail address: kaiying.wang@usn.no (K. Wang).

https://doi.org/10.1016/j.elecom.2023.107582
Received 23 August 2023; Received in revised form 11 September 2023; Accepted 13 September 2023
Available online 15 September 2023

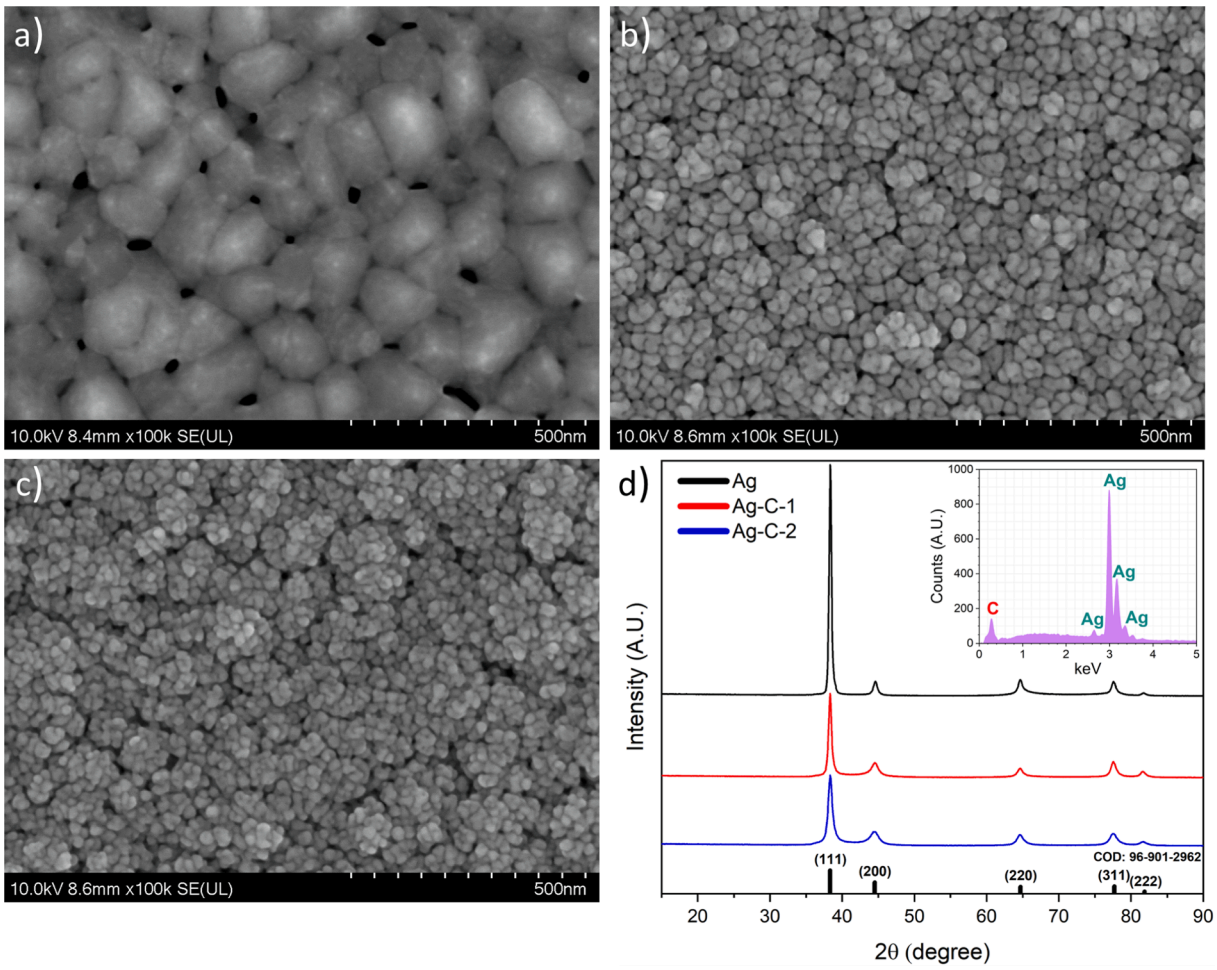

Fig. 1. SEM image of the a) Ag, b) Ag-C-1, and c) Ag-C-2 thin films. d) XRD patterns of the Ag and Ag-C films with inset of the EDX spectrum of Ag-C-2.

2. Methods

2.1. Catalyst synthesis

A 15 nm Chromium (Cr) adhesion layer was deposited onto soda lime glass pieces (3 × 0.5 cm^2) by e-beam deposition. The thin films were deposited by a magnetron co-deposition process with a direct current (DC) power of 100 W applied to the Ag target, while the radio frequency (RF) power of the C target was varied to synthesize two different Ag-C films: Ag-C-1 (350 W) and Ag-C-2 (500 W).

2.2. Material characterization

The XRD spectra were obtained using a Thermo Fisher Equinox 1000 low angle x-ray diffraction (XRD). The surface morphology and electron dispersive spectroscopy (EDX) analysis were performed using a Hitachi SU 8230 FE-SEM.

2.3. Electrochemical measurements

Electrochemical measurements were performed using an H-cell where the anodic and cathodic compartments were separated by a Nafion 117 proton exchange membrane. The chambers were filled with 75 mL of 0.5 M $KHCO_3$ electrolyte saturated with CO_2, having a pH of 7.4. iR compensation was conducted by observing the resistance versus the open circuit potential. All electrochemical measurements utilized a three-electrode configuration employing a Pt wire counter electrode and an Ag/AgCl (3 M KCl) reference electrode. Linear sweep voltammetry (LSV) curves were derived at a scan rate of 10 mV/s before and after saturating the electrolyte with CO_2. For the determination of the product selectivity each catalyst was tested at various potentials for 20 min, with fresh electrolyte used for every catalyst. The tests were repeated three times for each catalyst. Subsequently, all potentials were converted to the reversible hydrogen electrode (RHE) using the Nernst equation. The electrochemically active surface area (ECSA) was calculated from the double-layer capacitance (C_{DL}) which was extracted from cyclic voltammetry (CV) scans performed in the non-faradaic region of − 0.20 to − 0.35 V vs. RHE with scan rates of 50 – 250 mV/s. The C_{DL} was determined by calculating the linear fit of the difference between the cathodic and anodic current density at − 0.275 V vs. RHE as a function of the scan rate. The roughness factor (r_f) was calculated by dividing the C_{DL} value obtained for the Ag-C catalysts by that of the Ag reference. Finally, the ECSA was determined by multiplying the r_f with the geometric surface area of the catalyst. Gaseous reaction products were quantified using a Shimadzu-GC-2010 PLUS gas chromatograph (GC), featuring a ShinCarbonST column and a dielectric-barrier discharge ionization detector (BID). The gas was sampled every 20 min through an on-line configuration. The setup used for gas analysis has been reported previously [12].

3. Results and discussion

The surface morphology of the films as imaged by SEM can be seen in Fig. 1a-c. The pristine Ag film displays large grains with an average size of ~ 150 nm. However, when C is co-deposited with Ag, the particle size shrinks significantly, resulting in an average size of ~ 35 and ~ 25 nm

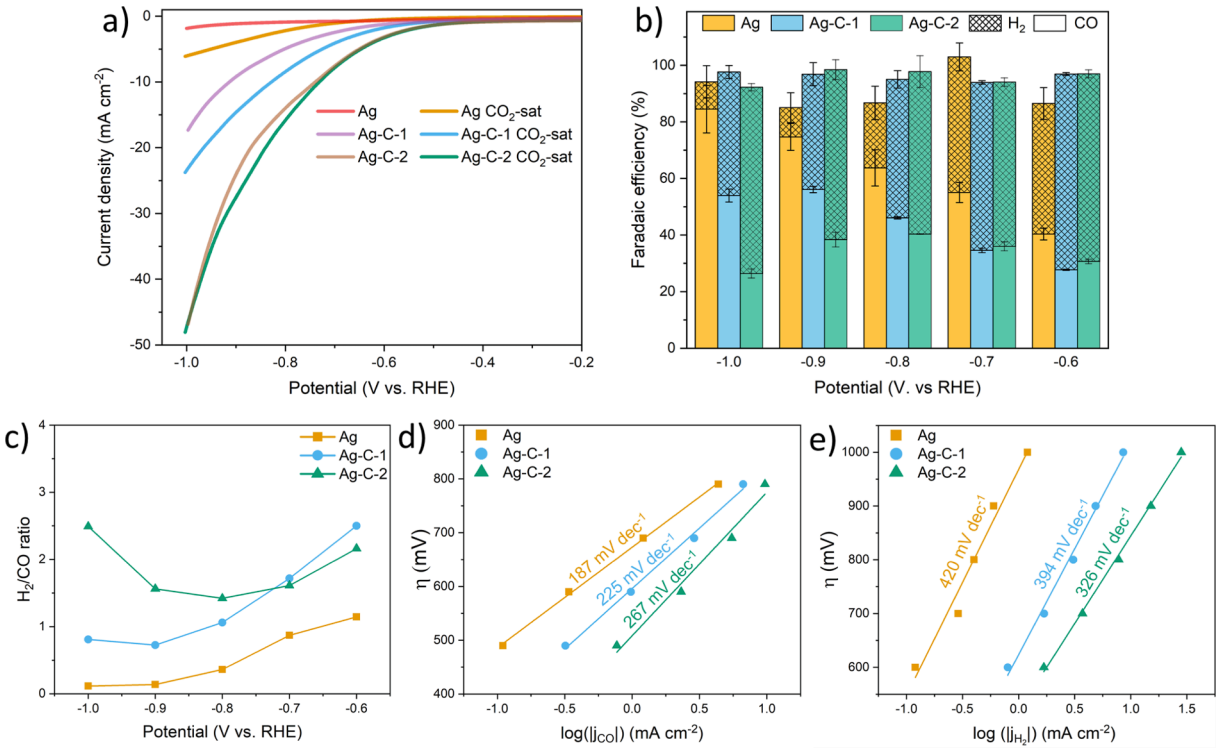

Fig. 2. Electrochemical characterization of the catalysts. a) LSV of the Ag and Ag-C catalysts, b) their product selectivity as a function of potential, c) the ratio of H_2/CO, the Tafel slope for d) CO formation and e) HER.

for the Ag-C-1 and Ag-C-2 films, respectively. Although the morphology for the Ag-C films is similar, the Ag-C-2 film consists of slightly smaller particles. EDX shows an increase in the C concentration from 2.3 at% for Ag to 7.6 and 13.4 at% for the Ag-C-1 and Ag-C-2 films, respectively. The small amount of C found in the pristine Ag film is likely due to C on the surface, but the EDX data provides an obvious trend in the C concentration with increasing RF sputtering power of the C target. The EDX spectrum obtained for the Ag-C-2 film can be seen in Fig. 1d inset. Next, the crystal structure of the films was investigated by XRD. The XRD pattern (Fig. 1d) of the sputtered Ag film displays a polycrystalline structure, with a high intensity Ag (1 1 1) peak. When C is co-sputtered with Ag, the Ag (1 1 1) peak intensity is reduced, and a broadening of the peaks can be observed, which results in a small bridge forming between the Ag (1 1 1) and Ag (2 0 0) peaks for the Ag-C-1 and Ag-C-2 films. The Debye-Scherrer equation was utilized to calculate the average crystallite size of the films by using the full-width half maximum (FWHM) of the Ag (1 1 1) peak. A crystallite size of 18.8 nm is calculated for pristine Ag, which is reduced to 14.0 nm for Ag-C-1, and further reduced to 9.5 nm for the Ag-C-2 film. Thus, the crystallite size is halved for the Ag-C-2 film relative to pristine Ag. The simultaneous reduction in particle size, crystallite size, and Ag (1 1 1) peak intensity suggests a disruption of the growth kinetics when co-sputtering with C due to the competitive growth of Ag and C during deposition. More precisely, an increase in the nucleation rate and suppressed growth of Ag leads to a reduction in particle and crystallite size. No shift in the diffraction angle of the Ag peaks that could indicate the placement of C in the Ag lattice was detected. Furthermore, no peaks associated with any C phase was detected, which could be due to the low concentrations relative to Ag, but more likely due to C exhibiting an amorphous structure.

Next, the catalytic performance of the films was determined by performing electrochemical CO_2 reduction in 0.5 M $KHCO_3$ with all potentials referenced to RHE. LSV scans reveal a substantial increase in current density for the Ag-C films that becomes larger when the C concentration is increased (Fig. 2a). Furthermore, when the electrolyte is saturated with CO_2, Ag and Ag-C-1 display enhanced current densities, whereas the difference before and after saturation is minor for Ag-C-2. For all the catalysts, CO and H_2 were the only gaseous reaction products detected, with a total faradaic efficiency (FE) close to 100%. The FE obtained for CO and H_2 in the potential range of − 0.6 to − 1.0 V can be seen in Fig. 2b. Pristine Ag shows a steady increase in FE(CO) as the applied potential becomes more negative, reaching a peak FE(CO) of 84.5% at − 1.0 V. In comparison Ag-C-1 exhibits an overall lower FE (CO), with a peak of 56.1% at − 0.9 V, whereby a reduction in FE(CO) is observed when increasing the potential to − 1.0 V. A further reduction in FE(CO) is seen for Ag-C-2, with a peak FE(CO) of 40.4% at − 0.8 V. Thus, Ag-C shows a significant decrease in the selectivity towards CO_2 reduction in favor of HER, which becomes more pronounced at more negative potentials. The strong preference of the Ag-C-2 catalyst for HER could explain why saturating the electrolyte with CO_2 only resulted in minor variation in current density during LSV. Overall, the current densities are vastly increased for the Ag-C films, resulting in a larger partial current density of CO (J_{CO}) for the Ag-C catalysts at all potentials. It should be noted that the effect is more subtle at − 1.0 V due to the high selectivity of Ag towards CO at this potential compared to the Ag-C catalysts. The activity towards HER was substantially higher for Ag-C, with a partial current density of H_2 (J_{H2}) that was 28-fold larger for Ag-C-2 than for Ag at − 1.0 V. The H_2/CO ratio of the Ag and Ag-C films obtained within the applied potential range can be seen in Fig. 2c. It is observed that the Ag-C-1 display a slightly larger H_2/CO ratio than Ag-C-2 at − 0.6 V and − 0.7 V, but the ratio declines at more negative potentials in a similar fashion to the Ag reference. On the other hand, Ag-C-2 show a parabolic curve for the H_2/CO ratio as a function of the applied potential, with start- and end points offering a H_2/CO ratio close to 2, which is ideal for the Fischer Tropsch and direct methanol synthesis. In comparison, the Ag reference catalyst obtains a H_2/CO ratio of 1.14 at − 0.6 V that rapidly decreases to 0.12 at − 1.0 V. These results show that the H_2/CO ratio appears to be tunable by first controlling the C concentration introduced into the films during co-deposition, and secondly by controlling the applied potential. From the Tafel slopes for the CO_2 reduction plotted in Fig. 2d, Ag exhibits a slope of 187 mV/dec, which

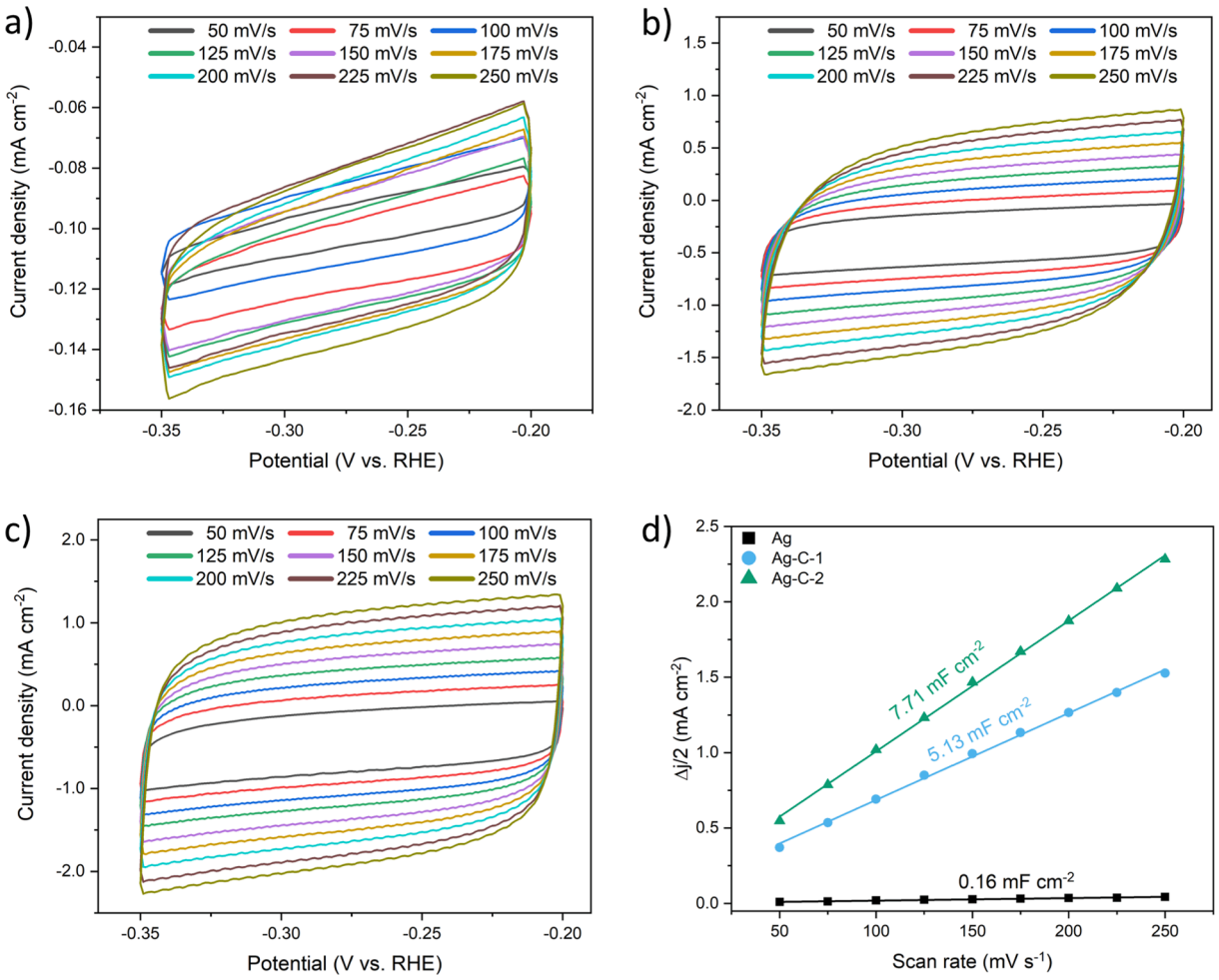

Fig. 3. CV scans performed at various scan rates for a) Ag, b) Ag-C-1, and c) Ag-C-2. d) C_{DL} slopes obtained from the CV scans in a)-c).

increases to 225 mV/dec for Ag-C-1 and 266 mV/dec for the Ag-C-2 catalyst. On the other hand, the Tafel slope for HER was reduced by ~ 100 mV/dec for the Ag-C-2 catalyst relative to Ag (Fig. 2e). Thus, the electrochemical CO_2 reduction becomes more sluggish while HER shows improved kinetics with increasing concentrations of C. It is well known that C does not contribute towards the CO2RR but have a proven capability of HER in a $KHCO_3$ electrolyte [13]. Therefore, an increase in C relative to Ag would favor HER over CO_2 reduction. Other factors that could enhance the selectivity towards HER is the reduction in Ag particle size, which in transition-metals have shown to increase both current densities and HER selectivity due to exhibiting a larger amount of edge and corner sites [5,14,15]. However, these particle size effects have been reported primarily for nanoparticles which are significantly smaller than the ones observed for the Ag-C films (<10 nm). Thus, the contribution of these morphological effects on the selectivity is considered minor in comparison to C. As the increase in J_{CO} could not be attributed to improved kinetics for the CO_2 reduction, it was believed that an increase in the surface area due to the porosity introduced by C could be responsible. Thus, a set of CV scans were performed at various scan rates in the range − 0.2 to − 0.35 V as seen in Fig. 3a-c to extract the C_{DL}, which was used to determine the ECSA. A significant increase is seen in the C_{DL}, from 0.16 mF/cm^2 for Ag, to 5.13 mF/cm^2 for Ag-C-1 and 7.71 mF/cm^2 for Ag-C-2 (Fig. 3d). The r_f relative to the pristine Ag film was 32 and 48 for Ag-C-1 and Ag-C-2, respectively. This corresponded to an ECSA of 0.75 cm^2 (Ag), 27 cm^2 (Ag-C-1), and 36 cm^2 (Ag-C-2), making the ECSA vastly larger for the Ag-C films, which explains the substantial increase in current density. The increase in ECSA results in a reaction rate that is significantly larger compared to the Ag nanowires at C sheets reported by Cho et.al [16], which achieved a similar H_2/CO ratio of syngas by varying the Ag nanowire loading. In terms of reaction rate and ability to tune the syngas ratio the performance of the Ag-C thin films is more comparable to the nanostructured Ag mesh reported by Lim et. al. [17]. However, from a cost-perspective the Ag-C thin films are more attractive since the overall material consumption can be reduced.

4. Conclusion

Ag-C composite catalysts were synthesized through a co-sputtering process using an Ag and C sputtering target. The co-deposition of C with Ag reduced the particle size from ~ 150 nm to < 40 nm while also reducing the crystallite size due to an increase in the nucleation rate that suppresses Ag growth. The Ag-C films display a significant increase in reaction rate relative to Ag, where the overall selectivity for CO is reduced in favor of HER. The increase in the ECSA for the Ag-C films due to the smaller particle size and porous nature of C make the Ag-C films capable of achieving large current densities due to an abundance of active sites, where the H_2/CO ratio can be tuned by adjusting the C concentration of the film. The combined ability to control the H_2/CO ratio while allowing for large geometric current densities makes the Ag-C an attractive syngas catalyst.

CRediT authorship contribution statement

Kim Robert Gustavsen: Conceptualization, Methodology, Investigation, Visualization, Writing – original draft. **Erik Andrew**

Johannessen: Supervision, Writing – review & editing. **Kaiying Wang:** Supervision, Funding acquisition, Writing – review & editing.

Declaration of Competing Interest

The authors declare that they have no known competing financial interests or personal relationships that could have appeared to influence the work reported in this paper.

Data availability

Data will be made available on request.

Acknowledgements

The authors K.R.G. and K.W. acknowledge the research grants from EEA (European Economic Area)-Norway-Romania project #Graftid, RO-NO-2019-0616 and EEA-Poland-NOR/POLNORCCS/ PhotoRed/0007/ 2019-00. K.R.G acknowledge support from the Norwegian Micro- and Nano- Fabrication Facility (NorFab, No. 245963/F50) and the strategic research plan of the University of South-Eastern Norway.

References

[1] D.B. Pal, R. Chand, S.N. Upadhyay, P.K. Mishra, Performance of water gas shift reaction catalysts: A review, Renew. Sustain. Energy Rev. 93 (2018) 549–565.
[2] B.M. Tackett, J.H. Lee, J.G. Chen, Electrochemical Conversion of CO2 to Syngas with Palladium-Based Electrocatalysts, Acc. Chem. Res. 53 (2020) 1535–1544.
[3] Y. Hori, H. Wakebe, T. Tsukamoto, O. Koga, Electrocatalytic process of CO selectivity in electrochemical reduction of CO2 at metal electrodes in aqueous media, Electrochim. Acta 39 (1994) 1833–1839.
[4] J.H. Lee, S. Kattel, Z. Jiang, Z. Xie, S. Yao, B.M. Tackett, W. Xu, N.S. Marinkovic, J. G. Chen, Tuning the activity and selectivity of electroreduction of CO2 to synthesis gas using bimetallic catalysts, Nat. Commun. 10 (2019) 3724.
[5] H. Mistry, R. Reske, Z. Zeng, Z.-J. Zhao, J. Greeley, P. Strasser, B.R. Cuenya, Exceptional Size-Dependent Activity Enhancement in the Electroreduction of CO2 over Au Nanoparticles, J. Am. Chem. Soc. 136 (2014) 16473–16476.
[6] W. Xi, R. Ma, H. Wang, Z. Gao, W. Zhang, Y. Zhao, Ultrathin Ag Nanowires Electrode for Electrochemical Syngas Production from Carbon Dioxide, ACS Sustain. Chem. Eng. 6 (2018) 7687–7694.
[7] M.A. Farkhondehfal, S. Hernández, M. Rattalino, M. Makkee, A. Lamberti, A. Chiodoni, K. Bejtka, A. Sacco, F.C. Pirri, N. Russo, Syngas production by electrocatalytic reduction of CO2 using Ag-decorated TiO2 nanotubes, Int. J. Hydrogen Energy 45 (2020) 26458–26471.
[8] Y.E. Kim, B. Kim, W. Lee, Y.N. Ko, M.H. Youn, S.K. Jeong, K.T. Park, J. Oh, Highly tunable syngas production by electrocatalytic reduction of CO2 using Ag/TiO2 catalysts, Chem. Eng. J. 413 (2021), 127448.
[9] L. Zeng, J. Shi, H. Chen, C. Lin, Ag Nanowires/C as a Selective and Efficient Catalyst for CO2 Electroreduction, Energies 14 (2021) 2840.
[10] J. Hong, K.T. Park, Y.E. Kim, D. Tan, Y.E. Jeon, J.E. Park, M.H. Youn, S.K. Jeong, J. Park, Y.N. Ko, W. Lee, Ag/C composite catalysts derived from spray pyrolysis for efficient electrochemical CO2 reduction, Chem. Eng. J. 431 (2022), 133384.
[11] F. Sastre, M.J. Muñoz-Batista, A. Kubacka, M. Fernández-García, W.A. Smith, F. Kapteijn, M. Makkee, J. Gascon, Efficient Electrochemical Production of Syngas from CO2 and H2O by using a Nanostructured Ag/g-C3N4 Catalyst, ChemElectroChem 3 (2016) 1497–1502.
[12] K.R. Gustavsen, E.A. Johannessen, K. Wang, Sodium Persulfate Pre-treatment of Copper Foils Enabling Homogenous Growth of Cu(OH)2 Nanoneedle Films for Electrochemical CO2 Reduction, ChemistryOpen 11 (2022) e202200133.
[13] M. Azuma, K. Hashimoto, M. Hiramoto, M. Watanabe, T. Sakata, Electrochemical Reduction of Carbon Dioxide on Various Metal Electrodes in Low-Temperature Aqueous KHCO 3 Media, J. Electrochem. Soc. 137 (1990) 1772.
[14] X. Deng, D. Alfonso, T.-D. Nguyen-Phan, D.R. Kauffman, Resolving the Size-Dependent Transition between CO2 Reduction Reaction and H2 Evolution Reaction Selectivity in Sub-5 nm Silver Nanoparticle Electrocatalysts, ACS Catal. 12 (2022) 5921–5929.
[15] R. Reske, H. Mistry, F. Behafarid, B. Roldan Cuenya, P. Strasser, Particle Size Effects in the Catalytic Electroreduction of CO2 on Cu Nanoparticles, J. Am. Chem. Soc. 136 (2014) 6978–6986.
[16] M. Cho, J.-W. Seo, J.T. Song, J.-Y. Lee, J. Oh, Silver Nanowire/Carbon Sheet Composites for Electrochemical Syngas Generation with Tunable H2/CO Ratios, ACS Omega 2 (2017) 3441–3446.
[17] J. Lim, H. Lim, B. Kim, S.M. Kim, J.-B. Lee, K.R. Cho, H. Choi, S. Sultan, W. Choi, W. Kim, Y. Kwon, Local pH induced electrochemical CO2 reduction on nanostructured Ag for adjustable syngas composition, Electrochim. Acta 395 (2021), 139190.